

## Diffusion model of solute dynamics in a membrane channel: Mapping onto the two-site model and optimizing the flux

Sergey M. Bezrukov

*Laboratory of Physical and Structural Biology, National Institute of Child Health and Human Development, National Institutes of Health, Bethesda, Maryland 20892-0924*

Alexander M. Berezhkovskii

*Mathematical and Statistical Computing Laboratory, Division for Computational Bioscience, Center for Information Technology, National Institutes of Health, Bethesda, Maryland 20892-0924*

Attila Szabo

*Laboratory of Chemical Physics, National Institute of Diabetes and Digestive and Kidney Diseases, National Institutes of Health, Bethesda, Maryland 20892-0924*

(Received 17 May 2007; accepted 3 July 2007; published online 19 September 2007)

The steady-state flux through a singly occupied membrane channel is found for both discrete and continuum models of the solute dynamics in the channel. The former describes the dynamics as nearest-neighbor jumps between  $N$  sites, while the latter assumes that the molecule diffuses in a one-dimensional potential of mean force. For both models it is shown that the flux is the same as that for a simple two-site model with appropriately chosen rate constants, which contain all the relevant information about the more detailed dynamics. An interesting consequence of single occupancy is that the flux has a maximum as a function of the channel-solute interaction. If this interaction is too attractive, the molecule will never leave the channel, thus blocking it for the passage of other molecules. If it is too repulsive, the solute molecule will never enter the channel. Thus the flux vanishes in the two limits and, hence, has a maximum somewhere in-between. In the framework of the diffusion model, we find the optimal intrachannel potential of mean force that maximizes the flux using the calculus of variations. For a symmetric channel this potential is flat and occupies the entire channel. In the general case of an asymmetric channel, the optimal potential is obtained by tilting the optimal flat potential for the corresponding symmetric channel around the channel center, so that the solute is driven towards the reservoir with the lower solute concentration by a constant force. This implies that the flux is higher when the solute binding near the channel exit is stronger than that near the entrance. [DOI: [10.1063/1.2766720](https://doi.org/10.1063/1.2766720)]

### I. INTRODUCTION

Membrane channels that allow metabolites or other macromolecular solutes to exchange between cells or different cell compartments are protein structures with water-filled pores. In this paper we consider the steady-state flux through a single channel in a membrane that separates two reservoirs with different concentrations of the solute. We assume that the channel can be occupied by at most one solute molecule, so that a molecule can enter only an empty channel, and once inside it blocks the channel. The major focus of our analysis is on how the interaction between the solute and the channel-forming protein affects the flux. To be more specific, we are looking for the interaction that maximizes the flux at a given concentration difference between the two reservoirs.

Traditionally large channels were thought to be “molecular sieves” which discriminate between different solutes based only on the solute size. In other words, they were regarded as low-selectivity structures that allow passage of the solute without any significant interaction with the channel pore. However, accumulating evidence<sup>1–13</sup> indicates that many such channels exhibit specific interactions with the solutes they have evolved to transport.

Recently Berezhkovskii and Bezrukov<sup>14,15</sup> have shown that solute attraction to the channel-forming proteins makes the transport through large solute-specific channels more efficient. They used the diffusion model introduced in Ref. 16 and explored in detail in Refs. 17 and 18 to describe the solute-pore interaction in terms of the potential of mean force. The attraction of the solute to the channel pore was modeled in terms of a square potential well that occupied the entire channel. The well depth that maximizes the flux was found as a function of the solute concentrations in the reservoirs, the solute diffusion coefficients in the channel and in the bulk, and the channel radius. It turns out that the optimal depth is independent of the channel length. It was shown that the smaller is the concentration, the deeper is the potential well. As the concentration increases, the depth decreases and, for very high solute concentrations, the depth is negative so that the optimal interaction is repulsive.<sup>15</sup> Kolomeisky<sup>19</sup> has recently shown that repulsive site-specific interaction increases the flux at sufficiently high concentrations also for the  $N$ -site model of the solute dynamics in the channel.

In this paper, in the framework of the diffusion model, we determine the optimal potential that maximizes the flux through a singly occupied channel without any *a priori* as-

assumptions about the shape of the potential. We begin by presenting a simple self-contained derivation of the general expression for the steady-state flux through a singly occupied channel. We show that the flux for the diffusion and multisite nearest-neighbor model of the solute dynamics in the channel is identical to the flux for a two-site model with appropriately chosen transition rates. Specifically, we find that jump rates between the two sites are equal to the reciprocal of the mean first passage times from one end of the channel to the other, calculated within the framework of the more detailed models. The site models of channel-facilitated membrane transport are frequently used in the literature because they combine conceptual simplicity with the ability to describe the main features of the transport found experimentally. The mapping of the diffusion and multistate models onto the two-site model, which is used to describe the steady-state flux through the channel, provides a microscopic interpretation of the phenomenological parameters of the two-site model.

As an application of this mapping we use it to find the optimal potential for a symmetric channel. Our analysis shows that the square-well potential occupying the entire channel, conjectured in Refs. 14 and 15, is indeed optimal when the channel is symmetric. However, the flux at given concentrations in the reservoirs can be further increased by making the channel asymmetric. Assuming that the intrachannel potential is arbitrary we use the calculus of variations to find the potential that maximizes the flux. The optimal potential in the general case turns out to be surprisingly simple. It can be obtained by tilting the optimal square-well potential of the corresponding symmetric channel around the center of the channel so that the optimal tilt drives the solute molecules towards the reservoir with the lower solute concentration by a constant force. An interesting implication of this result is that for a channel to function optimally, the solute attraction to the channel must be stronger on the side of the channel facing the reservoir to which solute molecules translocate. This finding is in contrast with a conjecture that the more pronounced binding takes place on the side of incoming solutes.<sup>20</sup>

Different models of the solute dynamics in the channel are schematically illustrated in Fig. 1. The simplest model of the steady-state flux through the channel that takes into account the solute dynamics in the channel [Fig. 1(a)] is completely characterized by six rate constants. Two of them describe the intrachannel transitions between the two sites,  $\alpha_+$  and  $\alpha_-$ , while the other rate constants,  $k_{in}^L$ ,  $k_{out}^L$ , and  $k_{in}^R$ ,  $k_{out}^R$ , describe the entrance and escape from the channel into the left ( $L$ ) and right ( $R$ ) reservoirs, respectively. A more general  $N$ -site model is shown in Fig. 1(b), and its continuum limit, the diffusion model, is shown in Fig. 1(c).

## II. FLUX AND MAPPING ONTO THE TWO-SITE MODEL

The simplest model of transport through a singly occupied channel that connects two reservoirs containing the transferring particles at concentrations  $c_L$  and  $c_R$ , which takes

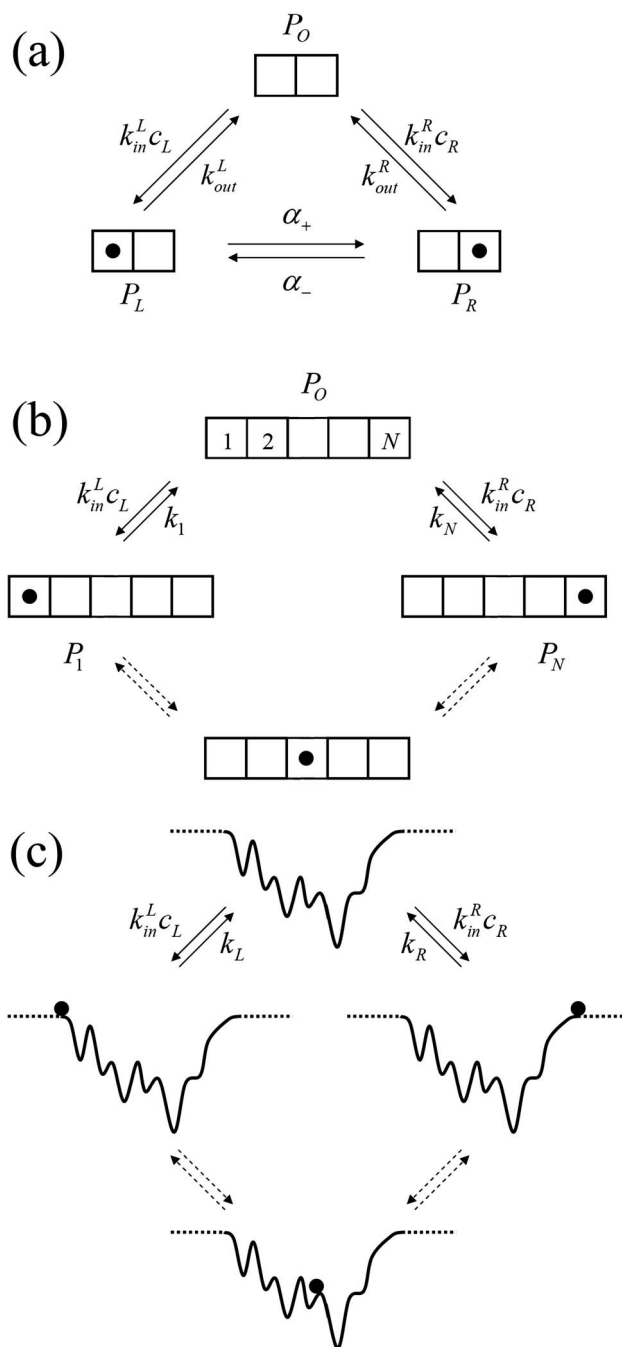


FIG. 1. Different models of the solute dynamics in the channel. (a) The two-site model. The rate constants for transitions between the two sites are  $\alpha_+$  and  $\alpha_-$  and for escape from the channel are  $k_{out}^L$  and  $k_{out}^R$ . (b) The  $N$ -site model. There are  $2(N-1)$  rate constants for the intrachannel transitions between neighboring sites and the rate constants  $k_1$  and  $k_N$  to describe the solute escape from the channel. (c) The diffusion model which is the continuous limit of the  $N$ -site model. The solute intrachannel dynamics is described as diffusion in the presence of a potential of mean force, while escape from the channel is described by imposing the radiation boundary conditions at the channel ends. Solid curves in this panel show the potential along the channel axis; dotted lines show the solute potential energy outside the channel. In all panels the black dot shows location of the solute in the channel. The solute entrance into the channel from the left and right reservoirs is described by the bimolecular rate constants  $k_{in}^L$  and  $k_{in}^R$ .

the particle intrachannel dynamics into account, is shown in Fig. 1(a). In this model the channel can be in three states, whose steady-state populations normalized to unity are denoted by  $P_O$ ,  $P_L$ , and  $P_R$ ,

$$P_0 + P_L + P_R = 1. \quad (1)$$

The steady-state flux  $J$ , defined as the difference between the average number of the particles passing through the channel from the left reservoir to the right one and the average number of the particles passing in the opposite direction, can be written as

$$J = \frac{\alpha_+ k_{\text{out}}^R k_{\text{in}}^L c_L - \alpha_- k_{\text{out}}^L k_{\text{in}}^R c_R}{\alpha_+ k_{\text{out}}^R + \alpha_- k_{\text{out}}^L + k_{\text{out}}^L k_{\text{out}}^R + k_{\text{in}}^L c_L (\alpha_+ + \alpha_- + k_{\text{out}}^R) + k_{\text{in}}^R c_R (\alpha_+ + \alpha_- + k_{\text{out}}^L)}. \quad (3)$$

Below we show that both the  $N$ -site and the diffusion models [Figs. 1(b) and 1(c)] can be mapped onto the two-site model. Specifically, the flux for these multistate models is given by Eq. (3) when the rate constants are chosen in accordance with the appropriate “microscopic” interpretation.

We begin with the diffusion model [Fig. 1(c)]. In this model the particle motion in the channel is described as one-dimensional diffusion in the presence of a potential of mean force  $U(x)$ , with position-dependent diffusion coefficient  $D_{\text{ch}}(x)$ , which may be quite different from the diffusion constant in the bulk. The steady-state distribution of the particle in the channel is described by the probability density  $p(x)$ ,  $x_L < x < x_R$ , where  $x_L$  and  $x_R$  are coordinates of the left and right boundaries of the channel [Fig. 1(c)]. The normalization condition analogous to that in Eq. (1) and the set of equations analogous to that in Eq. (2) are given by

$$P_0 + \int_{x_L}^{x_R} p(x) dx = 1, \quad (4)$$

$$\begin{aligned} J &= k_{\text{in}}^L c_L P_0 - \kappa_L p(x_L) \\ &= \kappa_R p(x_R) - k_{\text{in}}^R c_R P_0 \\ &= -D_{\text{ch}}(x) \frac{dp(x)}{dx} - D_{\text{ch}}(x) \beta \frac{dU(x)}{dx} p(x). \end{aligned} \quad (5)$$

Here  $\kappa_L$  and  $\kappa_R$  are rate constants describing escape from the channel of a particle approaching the boundary, and  $\beta = (k_B T)^{-1}$ , where  $k_B$  and  $T$  are the Boltzmann constant and the absolute temperature. The last expression in Eq. (5) gives  $J$  as a sum of the diffusive and drift fluxes. The latter is due to the force,  $-dU(x)/dx$ , acting on the particle in the channel.

It is convenient to write  $p(x)$  as a product of the dimensionless function  $\Phi(x)$  and the “equilibrium” density in the channel normalized to unity  $p_{\text{eq}}(x)$ ,

$$p(x) = \Phi(x) p_{\text{eq}}(x), \quad (6)$$

where

$$p_{\text{eq}}(x) = e^{-\beta U(x)} / Z, \quad Z = \int_{x_L}^{x_R} e^{-\beta U(x)} dx. \quad (7)$$

Then Eqs. (4) and (5) take the forms

$$J = k_{\text{in}}^L c_L P_0 - k_{\text{out}}^L P_L = k_{\text{out}}^R P_R - k_{\text{in}}^R c_R P_0 = \alpha_+ P_L - \alpha_- P_R. \quad (2)$$

Thus we have four unknowns,  $P_0$ ,  $P_L$ ,  $P_R$ , and  $J$ , and four linear equations. Solving them we find that the flux is given by

$$P_0 + \int_{x_L}^{x_R} \Phi(x) p_{\text{eq}}(x) dx = 1, \quad (8)$$

$$\begin{aligned} J &= k_{\text{in}}^L c_L P_0 - k_L \Phi(x_L) \\ &= k_R \Phi(x_R) - k_{\text{in}}^R c_R P_0 \\ &= -D_{\text{ch}}(x) p_{\text{eq}}(x) \frac{d\Phi(x)}{dx}, \end{aligned} \quad (9)$$

where

$$k_I = \kappa_I p_{\text{eq}}(x_I) = \kappa_I e^{-\beta U(x_I)} / Z, \quad I = L, R. \quad (10)$$

Function  $\Phi(x)$  can be found from Eq. (9) by simple integration,

$$\Phi(x) = \Phi(x_R) + J \int_x^{x_R} \frac{dx'}{D_{\text{ch}}(x') p_{\text{eq}}(x')}. \quad (11)$$

We use this  $\Phi(x)$  to write the normalization condition in Eq. (8) as

$$P_0 + \Phi(x_R) + J \tau_+ = 1, \quad (12)$$

where we have defined time  $\tau_+$  by

$$\tau_+ = \int_{x_L}^{x_R} p_{\text{eq}}(x) dx \int_x^{x_R} \frac{dx'}{D_{\text{ch}}(x') p_{\text{eq}}(x')}. \quad (13)$$

Changing the order of integration one can write this time in the form

$$\tau_+ = \int_{x_L}^{x_R} \frac{dx}{D_{\text{ch}}(x) p_{\text{eq}}(x)} \int_{x_L}^x p_{\text{eq}}(x') dx'. \quad (14)$$

This is the standard expression for the mean first passage time from  $x_L$  to  $x_R$  when the boundary at  $x = x_L$  is reflecting.<sup>21,22</sup> Note that this mean first passage time was not introduced on the basis of physical considerations but arose naturally. The mean first passage time in the opposite direction, i.e., from  $x_R$  to  $x_L$  when the boundary at  $x = x_R$  is reflecting,  $\tau_-$ , is

$$\tau_- = \int_{x_L}^{x_R} \frac{dx}{D_{\text{ch}}(x) p_{\text{eq}}(x)} \int_x^{x_R} p_{\text{eq}}(x') dx'. \quad (15)$$

The sum of the times  $\tau_+$  and  $\tau_-$  has a simple form,

$$\tau_+ + \tau_- = \int_{x_L}^{x_R} \frac{dx}{D_{\text{ch}}(x)P_{\text{eq}}(x)}. \quad (16)$$

We use this sum to write  $\Phi(x_L)$  obtained from Eq. (11) in the form

$$\Phi(x_L) = \Phi(x_R) + J(\tau_+ + \tau_-). \quad (17)$$

Using Eq. (17) we can write the normalization condition in Eq. (12) and Eq. (9) as

$$P_0 + \frac{\Phi(x_L)\tau_+ + \Phi(x_R)\tau_-}{\tau_+ + \tau_-} = 1, \quad (18)$$

$$\begin{aligned} J &= k_{\text{in}}^L c_L P_0 - k_L \Phi(x_L) \\ &= k_R \Phi(x_R) - k_{\text{in}}^R c_R P_0 = \frac{\Phi(x_L) - \Phi(x_R)}{\tau_+ + \tau_-}. \end{aligned} \quad (19)$$

Comparison of these equations with those in Eqs. (1) and (2) shows that one can map the diffusion model of the particle motion in the channel onto the two-site model by taking  $P_L = \Phi(x_L)\tau_+ / (\tau_+ + \tau_-)$  and  $P_R = \Phi(x_R)\tau_- / (\tau_+ + \tau_-)$  together with

$$\alpha_+ = \tau_+^{-1}, \quad \alpha_- = \tau_-^{-1}, \quad (20)$$

$$k_{\text{out}}^L = k_L(1 + \tau_-/\tau_+), \quad k_{\text{out}}^R = k_R(1 + \tau_+/\tau_-), \quad (21)$$

where  $k_L$  and  $k_R$  are defined in Eq. (10). Note that the rates of transitions between the two sites ( $\alpha_{+/-}$ ) turn out to be simply the reciprocals of the mean first passage times  $\tau_{+/-}$ . Relations in Eqs. (13)–(16) allow one to express the rate constants in Eqs. (20) and (21) in terms of  $U(x)$  and  $D_{\text{ch}}(x)$  that describe the interaction of the particle with the channel in the diffusion model. This mapping is analogous to that found by Kamp and Szabo<sup>23</sup> in the context of electron transfer between a donor and an acceptor undergoing conformational dynamics.

Thus we have shown that the steady-state flux for the diffusion model [Fig. 1(c)] is the same as the flux for the two-site model [Fig. 1(a)] with the rate constants given in Eqs. (20) and (21). This mapping means that as far as the flux is concerned, all information about the details of the particle dynamics in the channel can be packed into the mean first passage times from one end to the other and the equilibrium probabilities of being at the ends. All models for which these quantities are the same predict the same flux.

Using the relations in Eqs. (20) and (21) we can write the flux in Eq. (3) in terms of the mean first passage times between the channel ends given in Eqs. (14) and (15),

$$J = \frac{k_R k_{\text{in}}^L c_L - k_L k_{\text{in}}^R c_R}{(k_{\text{in}}^L c_L + k_L)(1 + \tau_+ k_R) + (k_{\text{in}}^R c_R + k_R)(1 + \tau_- k_L)}. \quad (22)$$

To our knowledge this result was first obtained on the basis of physically appealing arguments in Ref. 15 in the form [cf. Eqs. (1) and (6) from that paper]

$$J = \frac{P_{\text{tr}}^{L \rightarrow R} k_{\text{in}}^L c_L - P_{\text{tr}}^{R \rightarrow L} k_{\text{in}}^R c_R}{1 + k_{\text{in}}^L c_L t_{\text{inside}}^L + k_{\text{in}}^R c_R t_{\text{inside}}^R}. \quad (23)$$

Here  $P_{\text{tr}}^{L \rightarrow R}$  and  $P_{\text{tr}}^{R \rightarrow L}$  are the translocation probabilities which are the probabilities that the particle entering the channel from one side exits on the other, and the times  $t_{\text{inside}}^L$  and  $t_{\text{inside}}^R$  are the average lifetimes of particles entering the channel from the left and right reservoirs. General expressions for the translocation probabilities and for the average lifetimes are given in Eq. (3.14) of Ref. 17 and in Eq. (3.11) of Ref. 18, respectively. When these expressions are substituted into Eq. (23), the result in Eq. (22) is recovered.

Similarly, the  $N$ -site model [Fig. 1(b)] can also be mapped onto the two-site model. In this case,  $\tau_+$  and  $\tau_-$  are, respectively, the mean first passage times,  $\tau(1 \rightarrow N)$  and  $\tau(N \rightarrow 1)$ , between the two end sites of the channel when  $k_1$  and  $k_N$  are set equal to zero. These times can be found analytically for arbitrary site-to-site hopping rates. The rate constants  $k_L$  and  $k_R$  in Eq. (21) for the  $N$ -site model are given by  $k_L = k_1 P_{\text{eq}}(1)$  and  $k_R = k_N P_{\text{eq}}(N)$ , where  $P_{\text{eq}}(i)$  is the equilibrium distribution in the  $N$ -site channel normalized to unity. With this correspondence the steady-state flux for the  $N$ -site model is given by Eq. (22).

The expression in Eq. (22) is applicable both in the presence and in the absence of the potential drop between the reservoirs. Our further analysis is focused on the optimal potential  $U(x)$  that maximizes the flux which is due to the concentration difference in the absence of the potential drop. In this case the expression for the flux in Eq. (22) can be simplified using two relations. The first follows from the requirement that the flux vanishes at equilibrium when  $c_L = c_R = c$  and has the form  $k_R k_{\text{in}}^L = k_L k_{\text{in}}^R$  [see Eq. (22)]. The second relation follows from the fact that for a singly occupied channel  $k_{\text{in}}^I / k_I$ ,  $I = L, R$ , is just the equilibrium constant for “binding” a particle to the channel. Let  $V(x, y, z)$  be the potential energy of the particle at the point  $(x, y, z)$  inside the channel,  $x_L < x < x_R$ . If it is assumed that  $V(x, y, z) = 0$  outside,  $x < x_L$ ,  $x_R < x$ , then

$$\frac{k_{\text{in}}^I}{k_I} = \int_{x_L}^{x_R} dx \int \exp[-\beta V(x, y, z)] dy dz = AZ, \quad I = L, R, \quad (24)$$

where  $Z$  is the partition function defined in Eq. (7), and  $A$  is a constant with dimensions of area entering into the definition of the potential of mean force  $U(x)$ ,

$$\exp[-\beta U(x)] = \frac{1}{A} \int \exp[-\beta V(x, y, z)] dy dz, \quad x_L < x < x_R. \quad (25)$$

Using these relations we can write the flux in Eq. (22) as

$$\frac{c_L - c_R}{J} = \frac{1}{k_{in}^L} + \frac{1}{k_{in}^R} + \frac{\tau_+ + \tau_-}{AZ} + \left( \frac{c_L}{k_{in}^R} + \frac{c_R}{k_{in}^L} \right) AZ + c_L \tau_+ + c_R \tau_- \quad (26)$$

This will be used in Section IV to find the optimal  $U(x)$  that maximizes the flux.

Transport of solutes that block the channel has been recently considered by Bauer and Nadler,<sup>24</sup> who obtained an expression for the steady-state flux using heuristic arguments. The authors, however, did not recognize that transport of solutes that blocks the channel is identical to transport through a singly occupied channel analyzed in Refs. 14 and 15. They mistakenly claim that considerations in Refs. 14 and 15 “hold only for noninteracting particles” in spite of the fact that their Eqs. (21) and (22) for the flux are essentially the same as our Eq. (26), which in turn is a special case of Eq. (23), which was first derived in Ref. 15. Specifically, their Eqs. (21) and (22) can be recovered from Eq. (26) if we formally set  $A=1$  and make the following correspondence between our  $c_I, k_{in}^I, I=L, R, \tau_{+/-}, Z$  and their  $c_{1,2}, k_{-}^{(1,2)}, \tau, n, \Delta n$ :  $c_1=c_L, c_2=c_R, k_{-}^{(1)}=k_{in}^L, k_{-}^{(2)}=k_{in}^R, \tau=(\tau_+ + \tau_-)/2, n=Z/2$ , and  $\Delta n=(\tau_+ - \tau_-)Z/[2(\tau_+ + \tau_-)]$ .

Finally we note that when the potential  $V(x, y, z)$  is localized inside the channel, the rate constants  $k_{in}^I, I=L, R$ , for a channel with circular openings are given by the Hill formula,<sup>25</sup>  $k_{in}^I=4D_b r(x_I)$ , where  $D_b$  is the particle diffusion constant in the bulk and  $r(x_I)$  are the effective radii of the openings (e.g., for a spherical solute the difference between the radii of the channel openings and the solute). When the openings are noncircular one still can use  $k_{in}^I$  given by the Hill formula with the approximate effective radii given by  $[32A_{ch}(x_I)P_{ch}(x_I)/(2\pi^2)]^{1/3}$ , where  $A_{ch}(x_I)$  and  $P_{ch}(x_I)$  are the areas and perimeters of the openings.<sup>26</sup>

### III. OPTIMAL SYMMETRIC CHANNEL

Now we consider conditions when the flux through a channel occupied by at most one particle has a maximum. We begin with a symmetric channel for which  $k_{in}^L=k_{in}^R=k_{in}$ ,  $\alpha_+=\alpha_-=\alpha$ , and  $k_{out}^L=k_{out}^R=k_{out}$ . In this case the flux for the two-site model given in Eq. (3) can be written as

$$\frac{k_{in}(c_L - c_R)}{J} = 2 + \frac{k_{out}}{\alpha} + k_{in}(c_L + c_R) \left( \frac{2}{k_{out}} + \frac{1}{\alpha} \right). \quad (27)$$

This flux goes to zero as  $k_{out} \rightarrow 0$  and  $k_{out} \rightarrow \infty$  and thus must have a maximum for some value of  $k_{out}$ , denoted here by  $k_{out}^*$ . The flux vanishes as  $k_{out} \rightarrow 0$  because a particle entering the channel stays in the channel for a very long time blocking the channel for other particles. The flux vanishes as  $k_{out} \rightarrow \infty$  since in this limiting case an entering particle has no chance to go through the channel because it instantly comes back to the reservoir from which it entered.

The flux in Eq. (27) considered as a function of  $k_{out}$  has a maximum at  $k_{out}^*=k_{out}^*=\sqrt{2\alpha k_{in}(c_L + c_R)}$ . The maximal value of the flux through the symmetric channel  $J_{max}^{sym}$  is given by

$$J_{max}^{sym} = \frac{k_{in}(c_L - c_R)}{2(1 + \sqrt{k_{in}(c_L + c_R)/(2\alpha)})^2}. \quad (28)$$

This flux monotonically increases with  $\alpha$  and reaches the maximum when  $\alpha$  is as large as possible. Based on our mapping one can see that this happens when the mean first passage time between the channel ends is as small as possible [Eq. (20)]. When  $D_{ch}(x)=\text{const}=D_{ch}$ , this occurs when the intrachannel potential  $U(x)$  is flat. The presence of a potential barrier would increase the first passage time because the particle would have to climb uphill to overcome the barrier. The presence of a potential well would also increase this time because the particle would become trapped. The largest value of  $\alpha$ ,  $\alpha_{max}$ , can be found from Eqs. (14) and (20),  $\alpha_{max}=2D_{ch}/l^2$ , where  $l=x_R-x_L$  is the length of the channel. This leads to  $k_{out}^*=(2/l)\sqrt{D_{ch}k_{in}(c_L + c_R)}$ .

Thus we have shown that the optimal potential for a symmetric channel is a square-well potential that occupies the entire channel. The well energy  $U^*$  can be obtained by equating  $k_{out}^*$  with the expression for  $k_{out}$  that follows from Eqs. (21) and (24), namely,  $k_{out}=2k_{in}/(AZ)=2k_{in}/(Al)\exp(\beta U)$ . Here we have used the fact that when the intrachannel potential  $U$  is a constant the partition function is  $Z=Al\exp(-\beta U)$ . In this way we find that the optimal energy  $U^*$  can be obtained from

$$\exp(2\beta U^*) = A^2 D_{ch}(c_L + c_R)/k_{in}. \quad (29)$$

For a cylindrical channel of radius  $r$  and cross section area  $A_{ch}=\pi r^2$  it is natural to choose  $A=A_{ch}$  so that the potential of mean force vanishes at the channel ends,  $U(x_L)=U(x_R)=0$  [Eq. (25)]. Then using  $k_{in}=4D_b r$  in Eq. (29) we arrive at

$$\exp(2\beta U^*) = \pi^2 D_{ch}(c_L + c_R) r^3 / (4D_b). \quad (30)$$

This result has been previously obtained in Refs. 14 and 15 using a different approach. It is interesting that the optimal well energy of the symmetric channel,  $U^*$ , is independent of the channel length. Finally, now we can write the flux in Eq. (28) in terms of the two concentrations,  $c_L$  and  $c_R$ , the geometric parameters of the channel,  $r$  and  $l$ , and the particle diffusion coefficients in the channel and in the reservoirs,  $D_{ch}$  and  $D_b$ .

For typical values of the parameters, the right-hand side of Eq. (30) is smaller than unity, and, hence,  $U^* < 0$ , so that the optimal potential is a square well. At concentrations, for which  $(c_L + c_R)r^3 > 4D_b/(\pi^2 D_{ch})$ , the right-hand side of Eq. (30) is greater than unity, and, hence,  $U^* > 0$ . For such extremely high concentrations [higher than 1M assuming that  $r=1$  nm and  $4D_b/(\pi^2 D_{ch})=1$ ], the optimal potential is a square barrier rather than a square well. The fact that the optimal potential can be repulsive rather than attractive at sufficiently high concentrations of the solute, mentioned in Ref. 15, has been recently discussed in detail by Kolomeisky<sup>19</sup> in the framework of the  $N$ -site model of the solute dynamics in the channel. In its simplest form, his analysis employs a single site model of the channel and assumes that a change in the energy of the channel site changes the rate of entering the channel (i.e.,  $k_{in}^I$ ). Here we have assumed that  $k_{in}^I$  are independent of the potential inside the

channel. A consequence of this distinction is that the optimal potential becomes repulsive at different concentrations in the two models.

#### IV. OPTIMAL ASYMMETRIC CHANNEL

Next we relax the symmetry requirement and find the optimal potential profile  $U_{\text{opt}}(x)$ ,  $x_L < x < x_R$ , for the more general case of an asymmetric channel assuming that  $D_{\text{ch}}(x) = \text{const} = D_{\text{ch}}$ . To do this we write the flux in Eq. (26) in terms of  $U(x)$  using the relations in Eqs. (7) and (14)–(16). The result is

$$\begin{aligned} \frac{c_L - c_R}{J} &= \frac{1}{k_{\text{in}}^L} + \frac{1}{k_{\text{in}}^R} + \frac{1}{AD_{\text{ch}}} \int_{x_L}^{x_R} e^{\beta U(x)} dx \\ &+ A \left( \frac{c_L}{k_{\text{in}}^R} + \frac{c_R}{k_{\text{in}}^L} \right) \int_{x_L}^{x_R} e^{-\beta U(x)} dx \\ &+ \frac{1}{D_{\text{ch}}} \int_{x_L}^{x_R} e^{\beta U(x)} dx \left[ c_L \int_{x_L}^x e^{-\beta U(x')} dx' \right. \\ &\left. + c_R \int_x^{x_R} e^{-\beta U(x')} dx' \right]. \end{aligned} \quad (31)$$

The right-hand side of Eq. (31) is a functional of the potential  $U(x)$ ,  $W[U(x)]$ . To find the potential that minimizes this functional and hence maximizes the flux, we expand  $W[U(x) + \delta U(x)]$  to linear order in  $\delta U(x)$ . This leads to  $W[U(x) + \delta U(x)] \approx W[U(x)] + \int_{x_L}^{x_R} \delta U(x') w(x') dx'$ , where function  $w(x)$  is called the functional derivative of  $W[U(x)]$ ,  $w(x) = \delta W[U(x)] / \delta U(x)$ . This function, in turn, is a functional of  $U(x)$ . For the optimal potential  $w(x) = 0$ . In this way we find that

$$\begin{aligned} w(x) &= \frac{1}{Ae^{-\beta U(x)}} - \frac{AD_{\text{ch}}}{k_{\text{in}}^L k_{\text{in}}^R} (k_{\text{in}}^L c_L + k_{\text{in}}^R c_R) e^{-\beta U(x)} \\ &+ c_L \left[ e^{\beta U(x)} \int_{x_L}^x e^{-\beta U(x')} dx' \right. \\ &\left. - e^{-\beta U(x)} \int_x^{x_R} e^{\beta U(x')} dx' \right] \\ &+ c_R \left[ e^{\beta U(x)} \int_x^{x_R} e^{-\beta U(x')} dx' \right. \\ &\left. - e^{-\beta U(x)} \int_{x_L}^x e^{\beta U(x')} dx' \right] = 0. \end{aligned} \quad (32)$$

Thus  $U_{\text{opt}}(x)$  is the solution of this equation.

Differentiating Eq. (32) with respect to  $x$  twice, we find that the optimal  $U(x)$  satisfies  $U''(x) = 0$  and hence can be written in the form

$$U_{\text{opt}}(x) = U - F(x - x_L - l/2), \quad x_L < x < x_R, \quad (33)$$

where  $U$  is the value of  $U_{\text{opt}}(x)$  at the center of the channel,  $x = x_L + l/2$ , and  $F$  is the tilt. The optimal values of  $U$  and  $F$  denoted by  $U^*$  and  $F^*$  can be found using Eq. (32). This leads to the following expression for the energy of the optimal potential in the center of the channel,  $U^*$ ,

$$\exp(2\beta U^*) = A^2 D_{\text{ch}} (k_{\text{in}}^L c_L + k_{\text{in}}^R c_R) / (k_{\text{in}}^L k_{\text{in}}^R). \quad (34)$$

The optimal tilt  $F^*$  can be found solving the equation

$$c_L \exp(-\beta F^* l/2) - c_R \exp(\beta F^* l/2) = \beta F^* \exp(\beta U^*) / A. \quad (35)$$

Using these relations in Eq. (31) we can write the maximum flux  $J_{\text{max}}$  as

$$\frac{c_L - c_R}{J_{\text{max}}} = \frac{1}{k_{\text{in}}^L} + \frac{1}{k_{\text{in}}^R} + \frac{c_L [1 + \beta F^* l - \exp(-\beta F^* l)] + c_R [1 - \beta F^* l - \exp(\beta F^* l)]}{D_{\text{ch}} (\beta F^*)^2}. \quad (36)$$

#### V. ILLUSTRATIVE CALCULATIONS

Our analysis has shown that the optimal intrachannel potential that maximizes the flux through a singly occupied channel is determined by the solute concentrations in the two reservoirs separated by the membrane. Usually these concentrations are quite different. With this in mind we set  $c_R = 0$ . We assume that the channel is a cylinder of radius  $r$  and again choose  $A$  in Eq. (25) equal to the channel cross section area,  $A = \pi r^2$ , so that  $U(x_L) = U(x_R) = 0$ . Using this and the Hill formula,  $k_{\text{in}}^L = k_{\text{in}}^R = k_{\text{in}} = 4D_b r$ , we can write Eqs. (34)–(36) as

$$\exp(2\beta U^*) = \pi^2 D_{\text{ch}} c_L r^3 / (4D_b), \quad (37)$$

$$(\beta F^* l)^2 \exp(\beta F^* l) = 4D_b c_L r l^2 / D_{\text{ch}}, \quad (38)$$

$$J_{\text{max}} = \frac{4D_b c_L r}{1 + (1 + \beta F^* l) \exp(\beta F^* l)}. \quad (39)$$

The maximum flux through the symmetric channel [Eq. (28)] in this case takes the form

$$J_{\text{max}}^{\text{sym}} = \frac{2D_b c_L r}{(1 + \sqrt{D_b c_L r l^2 / D_{\text{ch}}})^2}, \quad (40)$$

obtained earlier in Refs. 14 and 15. Note that Eq. (30) (with  $c_R = 0$ ), which determines the optimal value of the constant intrachannel potential for the symmetric channel, is identical to Eq. (37) which determines the optimal potential at the center of the asymmetric channel.

The two maximum fluxes,  $J_{\text{max}}$  and  $J_{\text{max}}^{\text{sym}}$ , have different behavior as functions of the dimensionless concentration  $\tilde{c}$

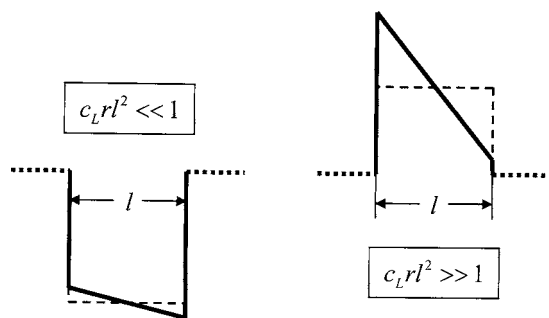


FIG. 2. Optimal intrachannel potentials of mean force at low and high concentrations of the solute in the left reservoir. Solid and dashed lines show the optimal potentials for asymmetric and symmetric channels, respectively, while dotted lines show the solute potential energy outside the channel. At low concentrations ( $c_L r l^2 \ll 1$ ,  $c_R = 0$ ) the optimal potential is a deep well which is almost flat even for an asymmetric channel (left panel). At high concentrations ( $c_L r l^2 \gg 1$ ,  $c_R = 0$ ) the optimal potential becomes a barrier which is strongly tilted towards the channel exit (right panel).

$= c_L r l^2$ . When  $\tilde{c} \rightarrow 0$  the energy  $U^*$  is negative and  $|\beta U^*| \gg 1$  while  $\beta F^* l \ll 1$ . This means that the optimal intrachannel potential is a deep well, which is practically flat (Fig. 2). Consequently, a particle entering the channel equilibrates inside the channel and escapes to the both reservoirs with equal probability  $1/2$ . Since the flux entering the channel is  $k_{in} c_L$ , the flux through the channel is  $k_{in} c_L / 2 = 2D_b r c_L$ , in agreement with Eqs. (39) and (40).

Both maximum fluxes are monotonically increasing functions of  $\tilde{c}$ . As  $\tilde{c} \rightarrow \infty$   $J_{max}^{sym}$  [Eq. (40)] saturates approaching the plateau value  $1/\tau_+$ , where  $\tau_+ = l^2 / (2D_{ch}) = \alpha_{max}^{-1}$  is the mean first passage time discussed earlier. On the other hand the maximum flux through an asymmetric channel tends to infinity as  $\tilde{c} \rightarrow \infty$  because the optimal tilt also tends to infinity,  $F^* \rightarrow \infty$  [Eq. (38)]. When  $\tilde{c} \rightarrow \infty$ , the energy  $U^*$  is positive (repulsive intrachannel potential),  $\beta U^* \rightarrow \infty$ , and the escape from the channel to the reservoir is a barrierless process.<sup>15,19</sup> In Fig. 2 we schematically show the optimal intrachannel potentials of mean force,  $U_{opt}(x)$ ,  $x_L < x < x_R$ , for asymmetric (solid lines) and symmetric (dashed lines) channels at low and high concentrations. Dotted lines show the potential  $V(x, y, z) = 0$  in the reservoirs outside the channel,  $x < x_L$  and  $x > x_R$ .

Figure 3 shows the flux in Eq. (31) as a function of  $\beta U$  and  $\beta F l / 2$  for a cylindrical channel of radius  $r = 1$  nm and length  $l = 5$  nm (these parameters reasonably describe the voltage-dependent anionic channel of mitochondrial outer membrane<sup>7</sup> when the size of the ATP molecule is taken into account) at  $c_L = 100$  mM,  $c_R = 0$ , and  $D_b = 2D_{ch} = 3 \times 10^{-10}$  m<sup>2</sup>/s. As follows from Eqs. (37) and (38), for this parameter set the flux reaches a maximum at  $\beta U^* \approx -1.3$  and  $\beta F^* l / 2 \approx 0.8$ .

In Fig. 4 we show the energies  $\beta U^*$  and  $\beta F^* l / 2$  found from Eqs. (37) and (38) as functions of the dimensionless concentration  $\tilde{c}$  for  $l/r = 5$  and  $D_b/D_{ch} = 2$ . The inserts, showing  $U_{opt}(x)$  at three values of  $\tilde{c}$ , illustrate how the optimal potential changes as the concentration increases.

## VI. CONCLUDING REMARKS

One of the main results of this paper is the mapping of the diffusion description of the particle intrachannel dynam-

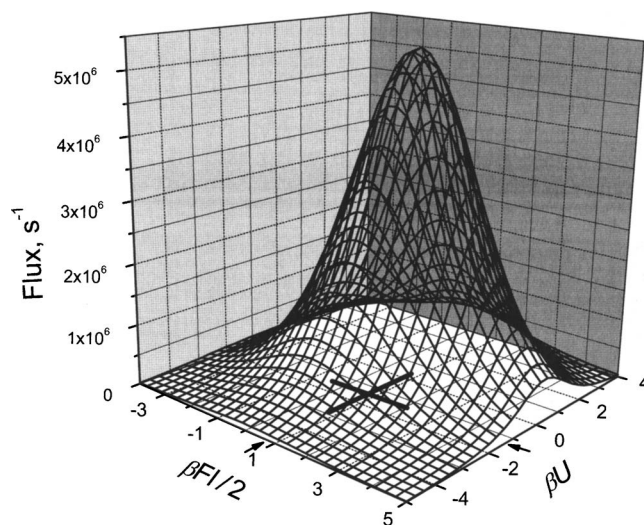


FIG. 3. The flux for  $U(x) = U - F(x - x_L - l/2)$ ,  $x_L < x < x_R = x_L + l$ , as a function of dimensionless energies  $\beta U$  and  $\beta F l / 2$  for a cylindrical channel of radius  $r = 1$  nm ( $A = \pi r^2$ ,  $k_{in}^L = k_{in}^R = 4D_b r$ ) and length  $l = 5$  nm at  $c_L = 100$  mM,  $c_R = 0$ , and  $D_b = 2D_{ch} = 3 \times 10^{-10}$  m<sup>2</sup>/s. The cross in the  $(\beta U, \beta F l / 2)$  plane shows the location of the maximum,  $\beta U^* \approx -1.3$ ,  $\beta F^* l / 2 \approx 0.8$ .

ics onto the two-site model. The transition rates for the two-site model can be chosen so that the steady-state flux found for the two-site model is equal to the flux found in the framework of the diffusion description. The resulting intersite hopping rates have a transparent physical interpretation since they turn out to be just the inverse mean first passage times between the channel ends. An analogous mapping holds for the multisite nearest-neighbor model of the solute dynamics in the channel. Thus all complex models with the same end-to-end mean first passage times and equilibrium probabilities at the channel ends predict the same flux. If one is interested only in the flux, the mapping onto the two-site model is exact. However, this does not imply that any other quantities obtained using the more detailed description of the particle intrachannel dynamics will be identical to those found in the framework of the equivalent two-site model.

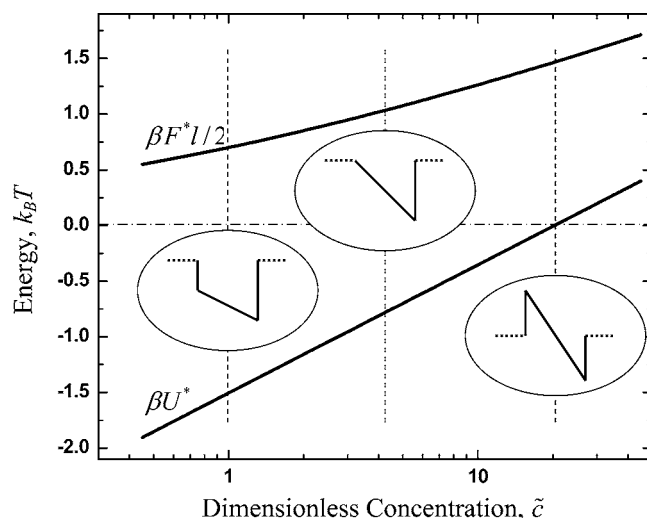


FIG. 4. The optimal energy at the center of the channel  $\beta U^*$  and the optimal tilt  $\beta F^* l / 2$  for  $l/r = 5$  and  $D_b/D_{ch} = 2$  as functions of the dimensionless concentration  $\tilde{c} = c_L r l^2$ . The inserts show how the optimal intrachannel potential of mean force changes as the concentration increases.

The second main result of this paper is the determination of the optimal intrachannel potential of mean force that maximizes the flux through a singly occupied channel when the flux is due to the difference in solute concentrations. The optimal potential drives the solute towards the reservoir with lower concentration (i.e., the channel “exit”). Thus it is preferable for a solute to “bind” more strongly near the exit rather than near the “entrance.” The optimum value of the interaction potential depends on the concentrations of the solute outside the channel. This suggests that in a given organism, channel proteins designed to transport the same molecule might have different amino-acid sequences. One gene might code for a channel protein that functions at high solute concentrations, while another for the one that works at low concentrations.

## ACKNOWLEDGMENTS

This study was supported by the Intramural Research Program of the NIH, Center for Information Technology, National Institute of Child Health and Human Development, and National Institute of Diabetes and Digestive and Kidney Diseases.

<sup>1</sup>M. Luckey and H. Nikaïdo, Proc. Natl. Acad. Sci. U.S.A. **77**, 167 (1980).

<sup>2</sup>R. Benz, A. Schmid, and G. H. Vos-Scheperkeuter, J. Membr. Biol. **100**, 21 (1987).

<sup>3</sup>T. Ferenci, BioEssays **10**, 1 (1989).

<sup>4</sup>H. Florke, F. P. Thinner, H. Winkelbach *et al.*, Biol. Chem. Hoppe Seyler

**375**, 513 (1994).

<sup>5</sup>R. Dutzler, Y.-F. Wang, P. J. Rizkallah, J. P. Rosenbusch, and T. Schirmer, Structure (London) **4**, 127 (1995).

<sup>6</sup>C. Andersen, M. Jordy, and R. Benz, J. Gen. Physiol. **105**, 385 (1995).

<sup>7</sup>T. K. Rostovtseva and S. M. Bezrukov, Biophys. J. **74**, 2365 (1998).

<sup>8</sup>L. Kullman, M. Winterhalter, and S. M. Bezrukov, Biophys. J. **82**, 803 (2002).

<sup>9</sup>E. M. Nestorovich, C. Danelon, M. Winterhalter, and S. M. Bezrukov, Proc. Natl. Acad. Sci. U.S.A. **99**, 9789 (2002).

<sup>10</sup>D. Lu, P. Grayson, and K. Schulten, Biophys. J. **85**, 2977 (2003).

<sup>11</sup>C. Danelon, E. M. Nestorovich, M. Winterhalter, M. Ceccarelli, and S. M. Bezrukov, Biophys. J. **90**, 1617 (2006).

<sup>12</sup>A. H. Delcour, Front. Biosci. **8**, 1055 (2003).

<sup>13</sup>H. Nikaïdo, Microbiol. Mol. Biol. Rev. **67**, 593 (2003).

<sup>14</sup>A. M. Berezhkovskii and S. M. Bezrukov, Biophys. J. **88**, L17 (2005).

<sup>15</sup>A. M. Berezhkovskii and S. M. Bezrukov, Chem. Phys. **319**, 342 (2005).

<sup>16</sup>S. M. Bezrukov, A. M. Berezhkovskii, M. A. Pustovoit, and A. Szabo, J. Chem. Phys. **113**, 8206 (2000).

<sup>17</sup>A. M. Berezhkovskii, M. A. Pustovoit, and S. M. Bezrukov, J. Chem. Phys. **116**, 9952 (2002).

<sup>18</sup>A. M. Berezhkovskii, M. A. Pustovoit, and S. M. Bezrukov, J. Chem. Phys. **119**, 3943 (2003).

<sup>19</sup>A. B. Kolomeisky, Phys. Rev. Lett. **98**, 048105 (2007).

<sup>20</sup>P. E. Klebba, Res. Microbiol. **153**, 417 (2002).

<sup>21</sup>A. Szabo, K. Schulten, and Z. Schulten, J. Chem. Phys. **72**, 4350 (1980).

<sup>22</sup>S. Redner, *A Guide to First-Passage Processes* (Cambridge University Press, New York, 2001).

<sup>23</sup>F. Kamp and A. Szabo, Cell Biophys. **12**, 145 (1988).

<sup>24</sup>W. R. Bauer and W. Nadler, Proc. Natl. Acad. Sci. U.S.A. **103**, 11446 (2006).

<sup>25</sup>T. L. Hill, Proc. Natl. Acad. Sci. U.S.A. **72**, 4918 (1975).

<sup>26</sup>O. K. Dudko, A. M. Berezhkovskii, and G. H. Weiss, J. Chem. Phys. **121**, 1562 (2004).